

Generating Quantum Random Numbers Using Entanglement in Low Earth Orbit

Ayesha Reezwana (✉ cqtayes@nus.edu.sg)

National University of Singapore <https://orcid.org/0000-0001-8172-1392>

Tanvirul Islam

National University of Singapore

Xueliang Bai

The university of Sydney

Christoph Wildfeuer

FHNW University of Applied Sciences and Arts Northwestern Switzerland

Alexander Ling

National University of Singapore

James Grieve

National University of Singapore <https://orcid.org/0000-0002-2800-8317>

Article

Keywords: Quantum, physical, Earth orbit, QRNG

Posted Date: July 27th, 2021

DOI: <https://doi.org/10.21203/rs.3.rs-690179/v1>

License:   This work is licensed under a Creative Commons Attribution 4.0 International License.

[Read Full License](#)

Generating quantum random numbers using entanglement in low Earth orbit

Ayesha Reezwana* and Tanvirul Islam

Centre for Quantum Technologies, 3 Science Drive 2, National University of Singapore, 117543 Singapore

Xueliang Bai

ARC Training Centre for CubeSats, UAVs, and Their Applications (CUAVA), School of Physics, The university of Sydney

Christoph F. Wildfeuer

FHNW University of Applied Sciences and Arts Northwestern Switzerland, School of Engineering, 5210 Windisch

Alexander Ling

*Centre for Quantum Technologies, 3 Science Drive 2, National University of Singapore, 117543 Singapore and
Department of Physics, National University of Singapore, Blk S12, 2 Science Drive 3, 117551 Singapore*

James A. Grieve†

*Quantum Research Centre, Technology Innovation Institute, Abu Dhabi and
Centre for Quantum Technologies, 3 Science Drive 2, National University of Singapore, 117543 Singapore*

We describe the implementation of a quantum random number generator (QRNG) on-board a nanosatellite deployed to low Earth orbit (LEO). The generator samples shot noise from an entangled photon-pair source based on spontaneous parametric down conversion, linking the entropy of the QRNG to fluctuations in the vacuum field. We present analysis of data acquired in lab-based acceptance testing as well as on-orbit, and use the source to implement a prototype for an off-grid randomness beacon.

I. INTRODUCTION

Quantum random number generators (QRNGs) access the inherent randomness of quantum processes as a source of entropy, in order to produce an unbiased and unpredictable output. These devices have been shown to have many prospective use cases, notably in cryptography [1], simulation [2], telecommunications [3], and financial systems [4]. QRNGs may be particularly appropriate for small-scale and resource-constrained platforms, where other physical entropy sources are scarce.

In contrast to other physical random number generators, the unpredictability that is a natural consequence of quantum mechanics provides an abundant and uncomplicated source of randomness. Despite this relative availability, it is non-trivial to extract randomness from a quantum source due to the presence of technical noise arising from the imperfect nature of the measurement devices [5].

In recent years, there have been many successful demonstrations of quantum random number generators in laboratories [6–8], and several commercial products have entered the marketplace [9]. In this work, we describe the implementation of a quantum random number generator on an orbiting nanosatellite, SpooQy-1 [10]. In addition to the tasks noted previously, orbiting random number generators may find utilization in “prepare-and-measure” quantum key distribution (QKD) schemes [11], and can enable the implementation of a resource known as a randomness beacon [12]. While a number of randomness beacons are currently accessible via the

internet [12, 13], an orbiting beacon would be available to remote infrastructure with only sporadic, high-latency internet access (for example, monitoring stations connected via store-and-forward satellite services [14, 15]). Such installations could then make use of beacon pulses, for example in time-stamping algorithms to increase the integrity of record-keeping, or for auditable input to a sampling process [16].

The primary goal of the SpooQy-1 mission is to demonstrate a compact and sturdy entangled photon pair source in space; a stepping-stone towards the development of cost-effective satellite-to-ground or satellite-to-satellite QKD. Due to its status as a secondary mission objective, our QRNG implementation is based on measurements made on the same polarization entangled photon-pair source.

In this manuscript, we provide a brief overview of this instrument, along with the randomness extraction procedure and related experimental results. We assess the quality of the generated data using randomness testing suites (including the popular “Dieharder” package [17]) on a large volume of extracted random bits and validate the “Dieharder” test results using Kolmogorov-Smirnov test (KS test) [18]. Finally, we describe a proof-of-concept implementation of a secure public randomness beacon, and demonstrate the retrieval of beacon data via two distant ground stations, located in Switzerland and Singapore.

II. SOURCE DESIGN AND IMPLEMENTATION

SpooQy-1 demonstrates generation of polarization entangled photon-pairs via a violation of the CHSH inequality [20]. To this end, the satellite payload is equipped with a quantum light source compatible with the stringent constraints of the

* cqtayes@nus.edu.sg

† james.grieve@tii.ae

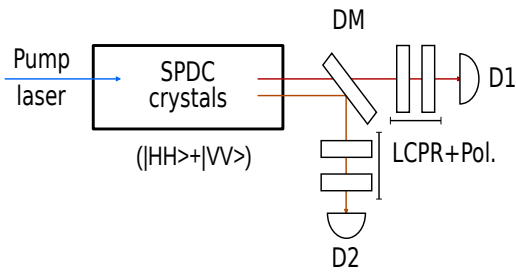


FIG. 1: A simplified block diagram of the random number generator, based on entangled photons generated via spontaneous parametric down conversion in nonlinear crystals (SPDC crystals). D1 and D2 represent detector systems that can perform polarization measurement using a combination of liquid crystal polarisation rotators (LCPR) and polarizing filters (Pol), on the photon-pairs after separation by a dichroic mirror (DM). A detection and counting circuit records the number of coincident events per second. The quantum shot noise of the coincident count is used as the entropy input to our QRNG.

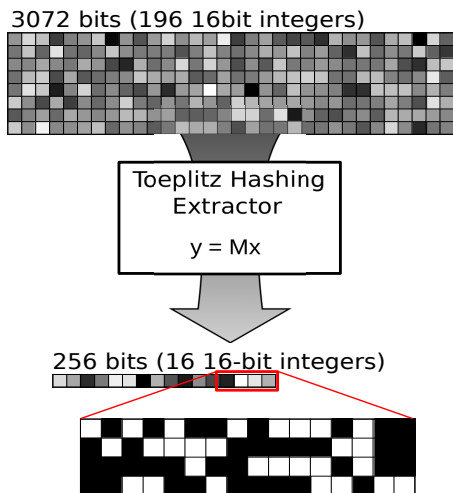


FIG. 2: A visualization of the random number extraction process. 256 uniform random bits (y) are generated from 3072 input bits (x), captured as 196 16-bit integers. The extraction is performed using a 256×3072 Toeplitz matrix [19] (M), which simultaneously removes any bias from the input sequence, and excludes the impact of non-quantum noise sources.

77 CubeSat bus [21], as well as a detector package capable of
 78 performing the required two-photon polarization correlation
 79 measurements. Detailed design of the source, analysis, and
 80 preliminary results can be found in the PhD dissertation of
 81 A. Villar [22].

82 Figure-1 shows a simplified block diagram of the entangled
 83 photon pair source and detection system. The source
 84 generates polarization entangled photons using spontaneous
 85 parametric down conversion (SPDC), a nonlinear optical
 86 process in which high energy photons with a small proba-
 87 bility split into pairs of lower energy photons following con-

88 servation of energy and momentum [23]. After separation by
 89 wavelength, two liquid crystal polarization rotators (LCPRs)
 90 are used to select measurement bases, with avalanche photo
 91 diodes (D1,D2) employed to detect individual photons. On-
 92 board electronics identify photon-pairs by selecting detec-
 93 tion events coincident within a 2 ns timing window [22].

94 Entangled photons are produced in Bell-like states such as

$$|\Phi^+\rangle = \frac{1}{\sqrt{2}}(|HH\rangle + |VV\rangle) \quad (1)$$

95 When the same measurement bases are selected for both
 96 photons, the majority of the coincident events are attributed
 97 to entangled photon pairs. Accidental coincidences attrib-
 98 uted to other sources (e.g. detector dark counts, stray
 99 light) are rendered negligible by the use of a sufficiently
 100 short timing window (in this work they account for $\sim 2\%$
 101 of the signal [22]). We select the diagonal basis to measure
 102 both of the photons. This re-enforces the quantum nature of
 103 the correlations, which for this geometry are approximately
 104 twice as strong as they would be in a classical device. As
 105 it is based on coincident events, this detection scheme can
 106 be used to minimize contribution from other entropy sources
 107 which would otherwise dominate the single detection chan-
 108 nels. Randomness in the resulting event rates originates from
 109 spontaneous vacuum fluctuations, and we use this signal as
 110 our raw entropy source.

111 The number of detected coincident events per unit time
 112 follows a Poisson distribution [24], with an easily character-
 113 ized mean value. We extract uniform random numbers from
 114 this signal using a Toeplitz hashing extractor [19]. Our ap-
 115 proach resembles work described by Sanguinetti et al. [5],
 116 where random numbers are generated by sampling a coher-
 117 ent illuminating beam with a mobile phone camera.

118 For a coincidence rate λ with X a random variable corre-
 119 sponding to the number of events observed in one second,
 120 the probability of observing a particular measurement n is
 121 given by

$$Pr[X = n] = \frac{e^{-\lambda} \lambda^n}{n!} \quad (2)$$

122 The quantum entropy corresponds to the min entropy of
 123 this distribution, given by

$$H_{\min}(X) = -\log_2 \left(\frac{e^{-\lambda} \lambda^{\lfloor \lambda \rfloor}}{\lfloor \lambda \rfloor!} \right) \quad (3)$$

124 While the contribution of classical noise is already limited
 125 in our implementation, in most cases, a properly designed
 126 randomness extractor is necessary to eliminate any informa-
 127 tion a hypothetical adversary might gain via knowledge or
 128 control over this classical noise component. Such an extrac-
 129 tor is also useful in distilling a uniform distribution from a
 130 Poissonian source, as in this case.

131 If k bits are used to encode each event X then from equa-
 132 tion (3) each such event has entropy at least $H_{\min}(X)$.

If each bit encoding X contains g bits of entropy then the randomness extraction ratio is,

$$g = \frac{H_{\min}(X)}{k} \quad (4)$$

133 Where, $g < 1$.

134 To extract random bits with unit entropy per bit we use a
135 Toeplitz hash based extractor. Here, a $l \times m$ Toeplitz matrix
136 M is used to extract l high entropy bits from m low entropy
137 bits, where l/m approaches the extraction ratio g .

138 If x is a Boolean vector of length m representing the low
139 entropy bits and y is the extracted l high entropy bits then,

$$y = Mx \quad (5)$$

140 Here, the Boolean vector x is constructed by concatenating
141 the binary encoding of several events drawn from the random
142 variable X so that the length m is achieved.

143 In this case, the output bits y are uniformly random with
144 probability [5]

$$1 - \varepsilon \geq 1 - 2^{-(gm-l)/2}. \quad (6)$$

145 Where, security parameter, $\varepsilon > 0$ is the probability of failure
146 for the randomness extraction.

147 In our experiment, coincidence data is encoded in $k = 16$
148 bit registers. From analysis of 47,422 seconds of data gener-
149 ated using a ground-based identical copy of the source,
150 we estimate the quantum randomness per bit as $g \geq 1/4$.
151 We employ a Toeplitz matrix with dimensions $l = 256$ and
152 $m = 3072$, yielding 256 bits of extracted randomness per 192
153 16-bit registers and achieving a rate of 80 bits/minute. From
154 equation (6) we expect the generated random bits to deviate
155 from perfect randomness with probability at most 2^{-256} .
156 This means that we must collect and process 2^{256} random
157 bits before being able to predict the next bit, assuming full
158 control over or knowledge of the classical noise of the original
159 source.

160 Figure 3(a) depicts detector coincident counts collected
161 for 125 minutes in a laboratory setting using a source identical
162 to that on the satellite. We see a slow moving trend (red line)
163 which we trace to gradual fluctuation of the power supply.
164 After removing the low frequency component using Fast Fourier
165 Transform (FFT) we obtain data exhibiting a Poisson distribu-
166 tion (mean 1785 and Fano factor [26] close to 1, Figure 3(c)).
167 This suggests that the remaining data consists of shot noise [5].
168 While resource constraints on the satellite do not permit the use
169 of FFT algorithms to remove the low frequency component, the
170 use of only short-duration data blocks (192 samples of the
171 coincident event rate) may enable us to disregard these low-
172 frequency contributions. This is confirmed by Figure 3(b), in
173 which Fano factors of 200-point data blocks are shown to be
174 close to 1, a signature of Poisson statistics reinforcing the
175 absence of significant low-frequency noise.

176 A 35.6 kB sequence of random data generated in the labo-
177 ratory is evaluated using the ‘‘Dieharder’’ test suite, and the
178

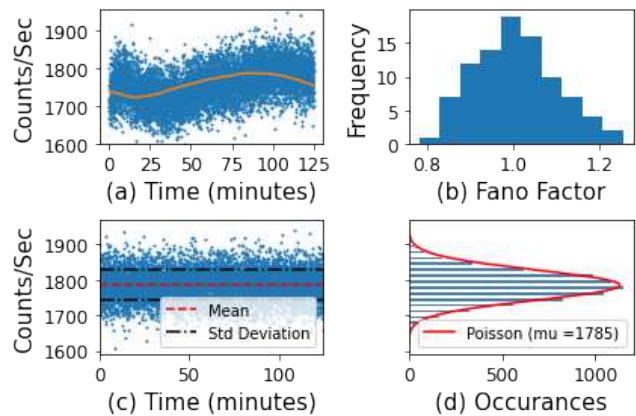


FIG. 3: Analysis of coincidence data obtained in a laboratory setting. (a) Raw coincident event rate and the moving average of the data points (red line) indicate the presence of a low frequency component to the noise. (b) Histogram of Fano factors taking 200 point blocks of the data, in which Poisson statistics are evident. (c) The same data after removing low frequency components by Fast Fourier Transform (FFT) filtering. (d) The filtered coincidence data fit to a Poisson distribution (red curve), indicating the remaining fluctuations are consistent with shot noise.

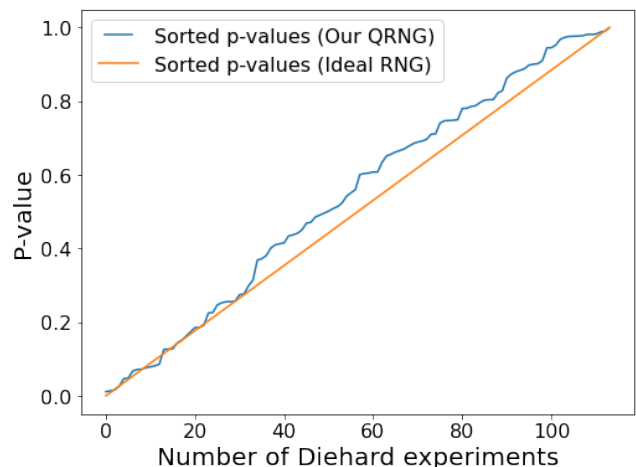


FIG. 4: Evaluating the (statistical) randomness of bits produced by our QRNG. Data generated in laboratory setup passes all tests in the ‘‘Dieharder’’ suite (i.e. $0.01 < p < 0.99$), illustrated here in the form of the KS test [18] (blue line) alongside a hypothetical ideal randomness source (orange line). This qualitative test sorts p values and plots them alongside values uniformly distributed over the interval $[0,1]$.

179 result validated by KS test with the analysis summarized
180 in Figure-4. In this analysis, the expectation for a random
181 source is that the p-value for each test should be distributed
182 in the interval $[0.01, 0.99]$. We use the KS test to confirm the
183 distribution of p-values and our source appears to conform to
184 the metric showing the empirically obtained p-values remain

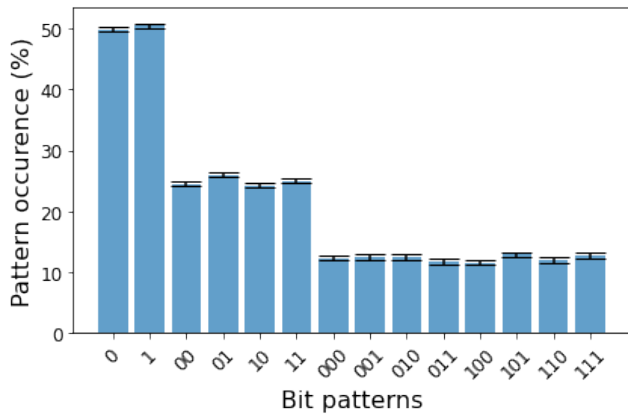


FIG. 5: Analysis of 66 runs containing total 16896 bits generated in orbit. For a limited data set of this size, tests such as “Dieharder” provide little meaningful insight. Instead, it is useful to compute the relative frequency of occurrence of all binary sub-strings of length 1, 2, 3, ... (the so-called Borel normality condition [25]). This analysis indicates a uniform distribution within error bars limited by finite sample size.

185 close to the theoretical ideal curve.

186 III. EXPERIMENT IN ORBIT

187 The experiment is repeated on-board SpooQy-1, after deployment in Low Earth Orbit. Due to the limited duty cycle of satellite operations and communication bandwidth we are restricted to retrieve at most 256 random bits per trial. It is non-trivial to analyze the randomness of such small datasets, for example, the “Dieharder” test is unsuitable [27]. However, one may estimate the quality of randomness of such short sequences of bits by observing the frequency of occurrence of sub-strings of a particular length (namely the Borel normality condition) [25], with a perfectly random sequence expected to produce a uniform distribution for each length. Figure-5 shows an analysis of 16896 random bits (i.e. the result of 66 trials), with the relative frequency matching this expectation. For example, asymptotically the occurrence of both 0 and 1 should be 50%, and the occurrence of each of the strings 00, 01, 10, and 11 should be 25%. In our analysis of 66 trials, the occurrence of 0 and 1 is 49.88(37)% and 50.50(37)% respectively. The sequences 00, 01, 10, and 11 were observed with frequencies 24.55(43)%, 26.06(47)%, 24.31(45)%, and 25.07(46)% respectively.

207 IV. PROTOTYPE RANDOMNESS BEACON

208 A randomness beacon is a public, periodically updated source of randomness provided as a resource for a variety of tasks which require a random input [12]. The beacon publishes “pulses” of random bits on a pre-defined schedule, which are typically broadcast over the internet.

213 We implemented a prototype randomness beacon with a
 214 24 hour refresh interval on-board the nanosatellite SpooQy-
 215 1, with the goal of demonstrating the feasibility of distribut-
 216 ing such a beacon to off-grid infrastructure. There are a few
 217 established functionality principles that a randomness beacon
 218 must satisfy in order to be useful [12]. These include the
 219 signing of each “pulse” using a public key traceable to the
 220 beacon originator, in order that the provenance of the beacon
 221 pulse can be confirmed. Pulses must also bear references
 222 to their parent in order to facilitate verification of the beacon’s
 223 integrity. While these features should be straightforward to
 224 implement on a dedicated satellite, SpooQy-1’s primary
 225 mission objectives laid stringent resource constraints
 226 on the QRNG subsystem. However, we were able to reinforce
 227 several standard elements of the satellite’s on-board
 228 radio to meet these requirements.

229 The on-board radio (Nanocom AX100, GOMspace)
 230 broadcasts a beacon signal at 30 second intervals, and is able
 231 to contain a simple data structure consisting of up to 256 generated
 232 random bits. The radio implements a hash-based message
 233 authentication code (HMAC), linking beacons to the
 234 satellite’s private key [28]. Alongside a timestamp, our data
 235 structure includes the current randomness beacon data in the
 236 form of 256 bits of full-entropy randomness. As computing
 237 a hash of the previous beacon data would be too computationally
 238 expensive for our highly constrained platform, we opt instead
 239 to include the full 256 random bits from the previous beacon,
 240 satisfying the requirement for linking to previous
 241 pulses.

242 The satellite beacon is encoded using a proprietary data
 243 format, which can be decoded by the GOMspace GS100
 244 ground station receiver [29]. Beacons were recorded at two
 245 ground-stations, located at Windisch (Switzerland) and on
 246 the National University of Singapore campus (Singapore).
 247 As our satellite was deployed from the ISS (International
 248 Space Station) orbit (inclination 51.6°, period ~90 minutes),
 249 we typically observe six passes per day over the Switzerland
 250 site, and up to four passes over the Singapore site. Since the
 251 two ground stations are in different time zones, it yields a
 252 possibility for us to receive the same beacon at two different
 253 stations approximately 10 times in 24 hours. Ground track,
 254 locations of our ground stations and randomness beacons received
 255 by the ground stations are shown in Figure 6.

256 As micro-satellite based broadband internet proliferates
 257 [30], there may be an increased demand for satellite based
 258 cryptographic infrastructure of this sort. To be truly
 259 useful, an orbital randomness beacon would require a higher
 260 refresh rate than demonstrated in this work (for example,
 261 the NIST beacon [12] updates every 60 s), robust cryptographic
 262 authentication and rigorous linking of sequential
 263 pulses [31]. While it was not possible to implement all of
 264 these on SpooQy-1, we believe that our proof of concept
 265 demonstration shows that such beacons can be hosted on-
 266 board low-resource satellites using existing technologies.

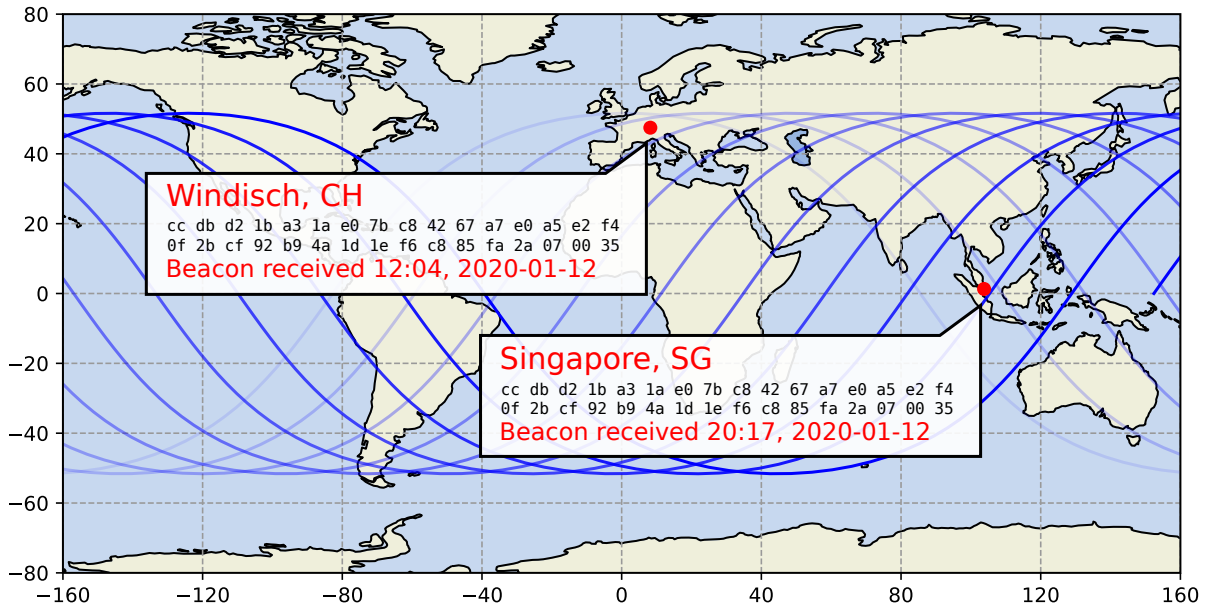


FIG. 6: Demonstration of a prototype orbiting randomness beacon. The ground track of our satellite is plotted against the world map, indicating the locations of our ground stations in Windisch (Switzerland) and Kent Ridge (Singapore). With an inclination of 51.6° and orbital period ~ 90 minutes, the satellite is able to communicate with both ground stations 10 times within a 24 hour period. As our prototype randomness beacon updates every 24 hours, we are able to confirm the reception of identical beacons at both locations.

V. CONCLUSION

In conclusion, we have implemented a quantum random number generator on-board an orbiting nanosatellite. As the entropy is derived from an entangled photon source, it may in future be possible to certify the quantum origin of the bits via the successful violation of the CHSH inequality.

As a proof of concept we demonstrate that quantum random number beacons can be implemented on-board nanosatellites using existing technologies. The burgeoning flourish of satellite based technologies in broadband network,

cryptographic infrastructure reinforces the necessity of establishing an orbiting public randomness beacon that leads to contribute in other promising applications such as in public lottery, voting protocols, contract signing and zero knowledge proofs.

ACKNOWLEDGEMENTS

This research was carried out at the Centre for Quantum Technologies, National University of Singapore, and supported by the National Research Foundation, Prime Minister's Office, Singapore under the grant NRFCRP12-2013-02.

-
- [1] W. Schindler, in *Cryptographic Engineering* (Springer, 2009) pp. 5–23.
- [2] W. K. Hastings, *Biometrika* **57**, 97 (1970).
- [3] L. Bello, *Debian open ssl predictable random number generator*, Tech. Rep. (Technical report, Debian. org, 2008).
- [4] B. Schneier, *Schneier's Cryptography Classics Library: Applied Cryptography, Secrets and Lies, and Practical Cryptography* (Wiley Publishing, 2007).
- [5] B. Sanguinetti, A. Martin, H. Zbinden, and N. Gisin, *Physical Review X* **4**, 031056 (2014).
- [6] L. Shen, J. Lee, J.-D. Bancal, A. Cerè, A. Lamas-Linares, A. Lita, T. Gerrits, S. W. Nam, V. Scarani, C. Kurtsiefer, *et al.*, *Physical review letters* **121**, 150402 (2018).
- [7] Y. Shi, B. Chng, and C. Kurtsiefer, *Applied Physics Letters* **109**, 041101 (2016).
- [8] M. Herrero-Collantes and J. C. Garcia-Escartin, *Reviews of Modern Physics* **89**, 015004 (2017).
- [9] “Quantum random number generators: A ten-year market assessment,” (2021), report IQT-QRNG-0121, Inside Quantum Technology.
- [10] A. Villar, A. Lohrmann, X. Bai, T. Vergoossen, R. Bedington, C. Perumangatt, H. Y. Lim, T. Islam, A. Reezwana, Z. Tang, *et al.*, *Optica* **7**, 734 (2020).
- [11] C. H. Bennett and G. Brassard, *Proceedings of IEEE International Conference on Computers, Systems and Signal Processing* **175**, 8 (1984).

- 313 [12] J. Kelsey, L. T. Brandão, R. Peralta, and H. Booth, *A ref-*
314 *erence for randomness beacons: Format and protocol version*
315 *2*, Tech. Rep. (National Institute of Standards and Technology,
316 2019).
- 317 [13] G. Wang and M. Nixon, in *2020 IEEE International Confer-*
318 *ence on Blockchain (Blockchain)* (IEEE, 2020) pp. 442–449.
- 319 [14] N. Hamamoto, Y. Arimoto, Y. Hashimoto, T. Ide, and
320 M. Sakasai, in *Proceedings of 1994 3rd IEEE International*
321 *Conference on Universal Personal Communications* (IEEE,
322 1994) pp. 418–422.
- 323 [15] M. Allery and J. Ward, in *3rd European Conference on Satel-*
324 *lite Communications-ECSC-3, 1993*. (IET, 1993) pp. 230–
325 235.
- 326 [16] A. Hevia and C. Gómez, *Communications of the ACM* **63**, 49
327 (2020).
- 328 [17] R. G. Brown, D. Eddelbuettel, and D. Bauer, *Open Source*
329 *software library*, under development (2013).
- 330 [18] F. J. Massey Jr, *Journal of the American statistical Association*
331 **46**, 68 (1951).
- 332 [19] X. Ma, F. Xu, H. Xu, X. Tan, B. Qi, and H.-K. Lo, *Physical*
333 *Review A* **87**, 062327 (2013).
- 334 [20] J. F. Clauser, M. A. Horne, A. Shimony, and R. A. Holt, *Phys-*
335 *ical review letters* **23**, 880 (1969).
- 336 [21] K. Durak, A. Villar, B. Septriani, Z. Tang, R. Chandrasekara,
337 R. Bedington, and A. Ling, in *Advances in Photonics of*
338 *Quantum Computing, Memory, and Communication IX*, Vol.
339 9762 (International Society for Optics and Photonics, 2016)
340 p. 976209.
- 341 [22] A. V. Zafra, *Building entangled photon pair sources for quan-*
342 *tum key distribution with nano-satellites*, PhD dissertation,
343 National University of Singapore (2019).
- 344 [23] D. C. Burnham and D. L. Weinberg, *Physical Review Letters*
345 **25**, 84 (1970).
- 346 [24] L. Mandel, *Proceedings of the Physical Society* **74**, 233
347 (1959).
- 348 [25] C. ian Caludet, in *Developments in Language Theory* (World
349 Scientific, 1993) p. 113.
- 350 [26] K. Rajdl, P. Lansky, and L. Kostal, *Frontiers in Computational*
351 *Neuroscience* **14** (2020).
- 352 [27] P. L’Ecuyer and R. Simard, *ACM Transactions on Mathemat-*
353 *ical Software (TOMS)* **33**, 1 (2007).
- 354 [28] *Ax100–Long-range software configurable VHF/UHF*
355 *transceiver*, GOMSPACE (2016).
- 356 [29] “*Nanocom gs100 datasheet*,” GOMSPACE; gs-ds-nanocom-
357 ax100-3.3.docx3.3; 12 August 2016.
- 358 [30] I. Levchenko, S. Xu, Y.-L. Wu, and K. Bazaka, *Nature As-*
359 *tronomy* **4**, 1012 (2020).
- 360 [31] M. J. Fischer, M. Iorga, and R. Peralta, in *Proceedings of*
361 *the International Conference on Security and Cryptography*
362 (IEEE, 2011) pp. 434–438.